

## Article

## Mixed Ligand Coordination Polymers for Metallogelation and Iodine Adsorption

Parthasarathi Dastidar, and Swapneswar Mondal

*Cryst. Growth Des.*, **Just Accepted Manuscript** • DOI: 10.1021/acs.cgd.8b01547 • Publication Date (Web): 04 Dec 2018Downloaded from <http://pubs.acs.org> on December 5, 2018

### Just Accepted

“Just Accepted” manuscripts have been peer-reviewed and accepted for publication. They are posted online prior to technical editing, formatting for publication and author proofing. The American Chemical Society provides “Just Accepted” as a service to the research community to expedite the dissemination of scientific material as soon as possible after acceptance. “Just Accepted” manuscripts appear in full in PDF format accompanied by an HTML abstract. “Just Accepted” manuscripts have been fully peer reviewed, but should not be considered the official version of record. They are citable by the Digital Object Identifier (DOI®). “Just Accepted” is an optional service offered to authors. Therefore, the “Just Accepted” Web site may not include all articles that will be published in the journal. After a manuscript is technically edited and formatted, it will be removed from the “Just Accepted” Web site and published as an ASAP article. Note that technical editing may introduce minor changes to the manuscript text and/or graphics which could affect content, and all legal disclaimers and ethical guidelines that apply to the journal pertain. ACS cannot be held responsible for errors or consequences arising from the use of information contained in these “Just Accepted” manuscripts.



# Mixed Ligand Coordination Polymers for Metallogelation and Iodine Adsorption

Swapneswar Mondal and Parthasarathi Dastidar\*

School of Chemical Sciences, Indian Association for the Cultivation of Science (IACS), 2A & 2B Raja S. C. Mullick Road, Jadavpur, Kolkata – 700032, West Bengal, India

*Coordination Polymers, Metallogels, Crystal Engineering, Supramolecular Gels, Nanoparticles, Iodine Adsorption*

**ABSTRACT:** A bis-pyridyl-bis-amide derivative of diphenyl methane (**L1**) and terephthalate (**TA**) were combined with a number of metal salts [Cu(II), Zn(II), Ni(II), Co(II) and Cd(II)] in 1:1:1 molar ratio to generate a series of coordination polymers (**CP1A-CP5**) which were thoroughly characterized by single crystal X-ray diffraction. All the CPs turned out to be lattice occluded crystalline solid having 4x4 grid framework structures. Under suitable conditions, the reactants of the corresponding CPs produced metallogels as envisaged considering a crystal engineering based structural rationale. One of the CPs, namely **CP5** demonstrated the ability to adsorb molecular iodine both in vapor and solution phase. Iodine adsorption was also found to be reversible as evident from its release in ethanol from both **CP5@I<sub>2</sub>** (vapor) and **CP5@I<sub>2</sub>**(solution). *In situ* synthesis of silver nanoparticles was also achieved in the gel matrix of **L1** without the help of any exogenous reducing agent.

**Introduction.** There have been increased research interests in developing rational approaches to design supramolecular gels<sup>1-6</sup> as they offer potential applications in various areas of material science.<sup>7-12</sup> Supramolecular gels are visco-elastic materials that comprise a small amount of gelator(s) and a large volume of solvent(s). Within a gel network formed due to supramolecular assembly of the gelator molecules (known as self-assembled fibrillar networks or SAFiNs<sup>13</sup>) the solvent molecules are immobilized due to surface tension or capillary force action resulting in a solid like materials called gels. Various non-covalent (supramolecular) interactions such as hydrogen bonding, halogen bonding,  $\pi$ - $\pi$  stacking, van der Waals interactions, charge transfer interactions etc. are responsible for the formation of SAFiNs. Metallogels<sup>14-16</sup> are supramolecular gels wherein metal-ligand coordination along with other supramolecular interactions takes part in SAFiNs. Coordination polymers (CPs),<sup>17,18,19</sup> coordination complexes (CCs),<sup>20-22</sup> cross-linked coordination polymers<sup>23</sup> are reported to form metallogels. Gels containing metal nanoparticles also belong to this class.<sup>24-26</sup>

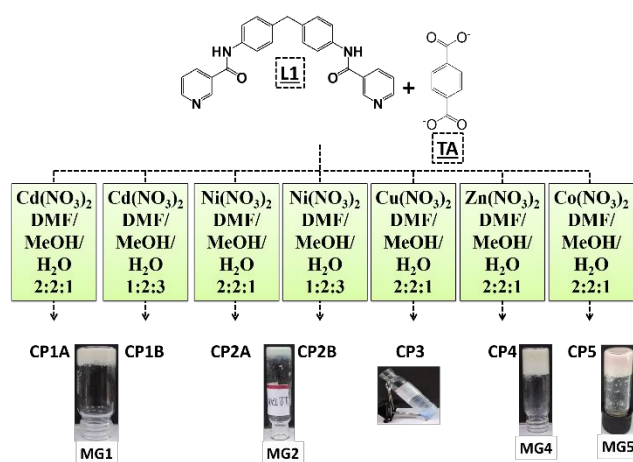
Gels are believed to be formed due to frustrated or failed crystallization process wherein a solution containing gelator molecules, under suitable conditions, takes a kinetically driven path towards meta-stable gels instead of thermodynamically stable crystals. In the absence of detail molecular level information of gelation mechanism, it is understandable that designing gelator molecule *a priori* is indeed a difficult task. Nevertheless, there have been efforts by various groups towards meeting this goal.<sup>27-30</sup> Our group has successfully

demonstrated the link between gels and crystal engineering<sup>31</sup>, and generated a large number of gels displaying intriguing functions by exploiting the merit of supramolecular synthons in the context of crystal engineering.<sup>32,33</sup> However, this approach is particularly valid for organogels wherein the solvent is organic and consequently do not participate in gel network formation. Metallogels, on the other hand, are usually formed in aqueous solvents and in here, water being good hydrogen bond donor as well as acceptor, do participate in gel network formation. This is quite evident from the crystal structure analysis of a number of hydrogelators.<sup>34-36</sup> We<sup>37,38</sup> and others,<sup>39</sup> therefore, proposed that compounds prone to form lattice occluded crystalline solids (LOCS) are potential target as gelators since in both LOCS and gel, a large number of solvent molecules are entrapped. Following this hypothesis, we have designed a number of metallogels that displayed intriguing functions.<sup>17</sup>

Iodine plays crucial role in the area of functional materials, biomedical applications, environmental chemistry etc.<sup>40,41</sup> For examples, applications of iodine and its isotopes are found in cancer treatment, and electrical conductivity.<sup>42,43</sup> Iodine isotopes pose an environmental hazard in nuclear affluent.<sup>44-48</sup> Therefore, demand for materials capable of adsorbing iodine has gained increased interest. Chalcogenide aerogels,<sup>49</sup> functionalized clays, and silver-based porous zeolitic materials<sup>50,51</sup> for iodine adsorption have been studied extensively. However, limited adsorption ability, high cost and environmental issues with these materials created demand for developing alternative materials. Coordination compounds such as CPs possess ability to adsorb iodine not only in its pore (for porous CPs) but

also the framework of CPs facilitates iodine adsorption through non-covalent interactions involving iodine and various sorption sites such as  $\pi$ -conjugated moiety, pyridyl, hydroxyl, ether, amino functionalities (encouraging halogen bonding) etc.<sup>52-61</sup>

With this background, we set out to synthesize a series of CPs by reacting a bis-pyridyl-bis-amide ligand having diphenylmethane backbone (**L1**), terephthalate (**TA**) and various metal ions [Cu(II), Zn(II), Ni(II), Co(II) and Cd(II)] in 1:1:1 molar ratio. While the expected 4x4 grid framework structure having hydrogen bond capable amide backbone of **L1** in the CPs is expected to occlude solvent molecules in its crystal lattice thereby forming LOCS, the aromatic  $\pi$  backbone of both the ligands (**L1** and **TA**) might help adsorb iodine. Therefore, the resulting CPs are expected to form metallogels under suitable conditions and also the CPs might have ability to adsorb iodine. We report the solvothermal synthesis of a series of CPs (**CP1A-CP5**) derived from **L1**, **TA** and the metal salts in DMF/methanol/water and their thorough characterization by single crystal X-ray diffraction (SXRD) (Scheme 1). All the CPs turned out to be LOCS as envisaged. Except the CP derived from Cu(II), all the other CPs displayed ability to form metallogel (**MG1**, **MG2**, **MG4** and **MG5**) in DMF/water (1:1 v/v) at room temperature. The Co(II) CP i.e. **CP5** displayed the ability to adsorb iodine both from solution as well as from vapor. Iodine adsorption by **CP5** was found to be reversible.



**Scheme 1.** Schematic representation of the synthesis of CPs and metallogels

**Results and Discussions.** Single crystals of the CPs obtained by solvothermal crystallization were subjected to SXRD (Table 1, see experimental section).

**Crystal structures of CP1A and CP1B.** The coordination polymers **CP1A** and **CP1B** were pseudopolymorphs because **CP1A** crystallized in the triclinic space group P-1 whereas **CP1B** displayed the orthorhombic space group Pbc<sub>a</sub> and the lattice occluded solvents were different in these cases; while **CP1A** contained three water and one MeOH (disordered around a center of inversion) as lattice occluded solvates, **CP1B** contained only one MeOH in the corresponding

asymmetric unit. The metal center in **CP1A** displayed a slightly distorted octahedral geometry wherein the axial sites were coordinated by two pyridyl N atoms of **L1** and the equatorial positions were occupied by O atoms of two **TA** (unidentate coordination mode) and two water molecules. On the other hand, Cd(II) in **CP1B** displayed pentagonal bipyramidal geometry; in here, the equatorial sites were occupied by O atoms of two **TA** (bidentate coordination mode) and one water molecule. The relative orientation of the terminal pyridyl N atoms in both the structures was *syn* whereas that of the amide carbonyl O atoms exhibited *anti* for **CP1A** and *syn* for **CP1B**. Both the ligands (**L1** and **TA**) were involved in extended coordination with Cd(II) metal center resulting in 2D grid network in both the structures; the grid architecture was corrugated 2D sheets for **CP1A** and 2D layered network for **CP1B**. The 2D networks were packed in parallel fashion in both the cases. Except the disordered MeOH, all the solvates (water) in **CP1A** were found to be stabilized in the crystal lattice by hydrogen bonding interactions involving the amide backbone of **L1**, metal bound water and themselves. In **CP1B**, on the other hand, the solvate MeOH was found to be tightly held in the crystal lattice through hydrogen bonding interactions involving amide functionality of **L1** (Figure 1 and 4).

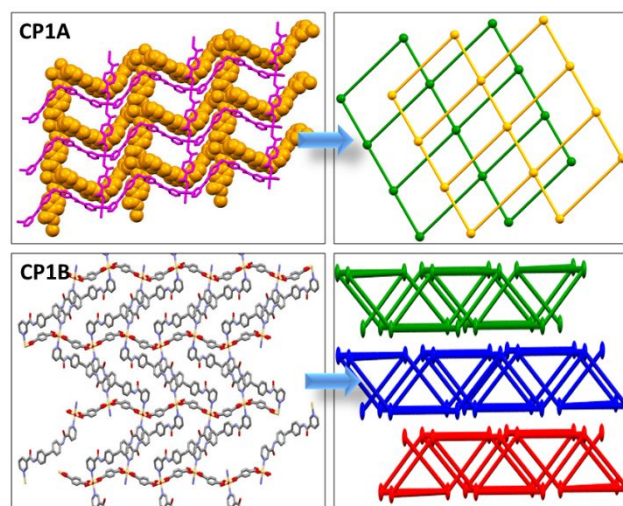


**Figure 1.** Crystal structure illustrations of **CP1A** and **CP1B** along with their corresponding network topology<sup>62,63</sup>

**Crystal structures of CP2A and CP2B.** Like **CP1A/CP1B**, these two CPs were also pseudopolymorphs as evident from their different space group (monoclinic C<sub>2/c</sub> for **CP2A** and P-1 for **CP2B**) and different lattice occluded solvate content (3H<sub>2</sub>O+MeOH for **CP1A** and 4H<sub>2</sub>O+MeOH for **CP2B**). The Ni(II) metal center in **CP2A** was located on a center of inversion thereby displaying perfect octahedral coordination environment; the axial positions were occupied by water molecules whereas the equatorial sites were coordinated by two O atoms of **TA** (unidentate coordination mode) and two N atoms of pyridyl moiety of **L1**. On the other hand, the metal center in **CP2B** showed slightly distorted octahedral geometry displaying identical coordination environment of **CP2A**.

The ligand **L1** adopted *anti-anti* and *anti-syn* conformation for **CP2A** and **CP2B**, respectively. The coordination network structures in both cases may best be described as 2D sheet that were packed in parallel fashion. The lattice occluded solvent molecules were found tightly held in the lattice via hydrogen bonding interactions with the amide backbone of the ligand **L1** (Figure 2 and 4).

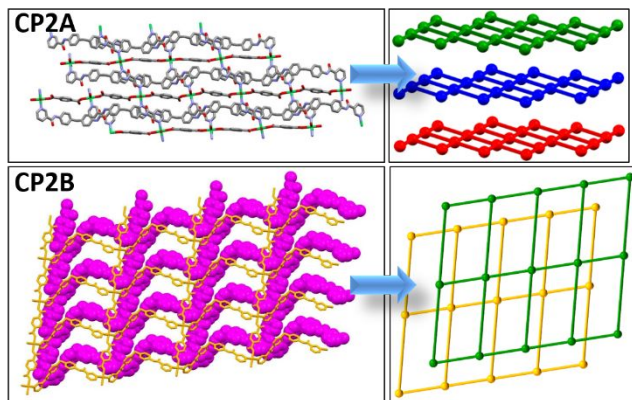


**Figure 2:** Crystal structure illustrations of **CP2A** and **CP2B** along with their corresponding network topology<sup>62,63</sup>

**Crystal structures of CP3, CP4 and CP5.** These CPs along with **CP2B** having identical space group (triclinic, P-1) and near identical cell dimensions (see Table 1) were isomorphous and therefore, they displayed identical crystal packing. The corresponding metal centers Cu(II), Zn(II) and Co(II) for **CP3**, **CP4** and **CP5**, respectively being located on a general position displayed slightly distorted octahedral geometry wherein the axial positions were occupied by water molecules and the equatorial sites were coordinated by two N atoms of **L1** and two O atoms of **TA** (unidentate coordination mode). The ligand **L1** adopted *anti-syn* configuration in all the cases as also observed in **CP2B**. The coordination networks were 2D sheet in all these structures. As expected, the lattice occluded solvents (3H<sub>2</sub>O, 3H<sub>2</sub>O+MeOH and H<sub>2</sub>O+MeOH for **CP3**, **CP4** and **CP5**, respectively) were found to be involved in hydrogen bonding with the amide backbone of the ligand **L1** (Figure 3 and 4).

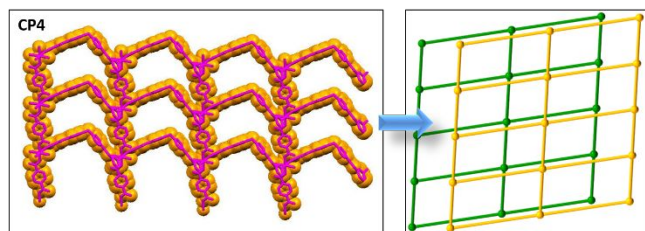


**Figure 3.** Crystal structure illustrations of **CP4** and the corresponding network topology<sup>62,63</sup>; **CP3** and **CP5** (being isomorphous to **CP4**) are not shown.

It may be mentioned that the crystalline phase purity of all the crystals was reasonably high as the simulated powder diffraction patterns matched well with that of the

experimental patterns obtained from bulk crystals (Figure S13-19, supporting information). Moreover, thermogravimetric analysis strongly supported the solvent content as observed in SXR analysis (Figure S20-26, supporting information).

Thus, isolation and characterization of these CPs clearly established that the network structures were 2D and the hydrogen bond capable backbone (amide) of **L1** played a crucial role in stabilizing the lattice occluded solvents through hydrogen bonding interactions as envisaged (Figure 4).

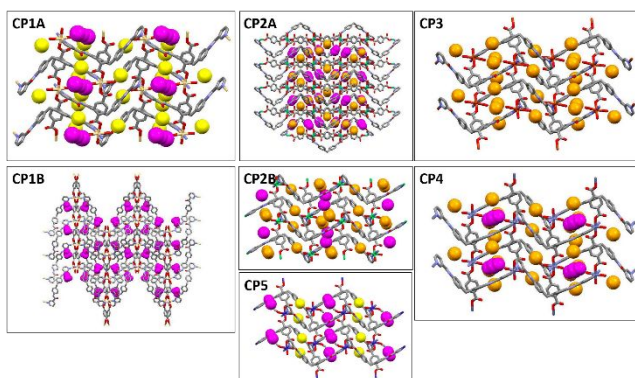


**Figure 4.** Illustration of crystal packing of all the CPs displaying lattice occluded solvents (color code: H<sub>2</sub>O – orange in **CP2A**, **CP2B**, **CP3** and **CP4**; H<sub>2</sub>O – yellow in **CP1A** and **CP5**; MeOH – magenta)

**Metallogelation.** The foregoing discussions on the crystal structures of the CPs clearly indicated that it was worthwhile to explore metallogelation with the reactants of the CPs i.e. **L1**, **TA** and the corresponding metal salts. Before exploring metallogelation, we first studied the gelation properties of **L1**. It turned out that **L1** was an excellent gelator of DMSO/water (3:2 v/v) with a minimum gelator concentration of 4 wt %. Guided by the crystal structures of the CPs, we reacted **L1**, **TA** and the corresponding metal salt in 1:1:1 molar ratio in DMF/water (1:1 v/v) that produced metallogels instantaneously after 5-10 minutes of sonication under ambient conditions except for Cu(NO<sub>3</sub>)<sub>2</sub> as evident from tube inversion test (Table 2, Scheme 1, see experimental section).

**Rheology.** More conclusive data were obtained when these metallogels were subjected to dynamic rheology (Figure 5). Gel being visco-elastic material is expected to display non Newtonian behavior in rheological studies. Frequency sweep plot wherein elastic modulus ( $G'$ ) and viscous or loss modulus ( $G''$ ) are plotted against the frequency ( $\omega$  rad/s) should typically display the following behavior for a gel sample: (a)  $G'$  must be much larger than  $G''$  and (b)  $G'$  should be frequency invariant throughout the entire frequency range. Frequency sweep data for the aqueous gel of **L1** and all the metallogels carried out at a fixed strain of 0.1 % (suggested by amplitude sweep experiments, Figure S31) displayed the characteristic signature of visco-elastic materials

confirming that they were indeed gels.  $\tan \delta$  ( $G''/G'$ ) values for all the gels were greater than 0.1 ( $\tan \delta$  0.23–0.42) indicating that the gels were significantly strong. The average  $G'$ 's in the linear visco-elastic region were within the range of ~2–237 kPa (Table 2).

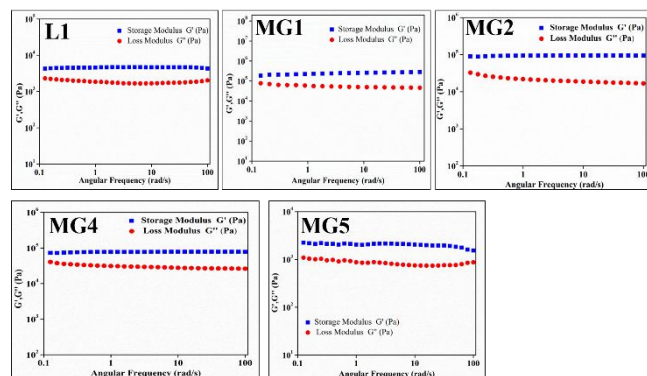


**Figure 5.** Frequency sweep plot for all the gels

**Microscopy.** To visualize the morphology of the gel network, we carried out TEM imaging of the dried gels (see experimental section). Several micrometer long plate like morphology was observed in the TEM images in dried gels of **L1**, **MG1** and **MG4**. Selected area electron diffraction (SAED) of the microplates observed under TEM did not show any diffraction confirming that they were not microcrystals precipitated out during TEM sample preparation. Although highly entangled fibrillar morphology is typical for supramolecular gels, such tape type of morphology as observed here is not uncommon (Figure 6).<sup>64</sup> It may be noted that TEM images of **MG2** and **MG5** could not be recorded due to the possible magnetic properties arising because of Ni(II) and Co(II) in the metallogel.

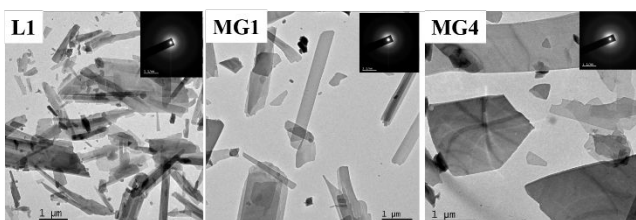


**Figure 6.** TEM images of the gels (inset – SAED).

**Iodine adsorption and release.** All the CPs were subjected to  $I_2$  adsorption both in vapor phase and in solution. Except **CP5**, all the CPs failed to show any  $I_2$  adsorption ability in both the phases as evident from visual observation. In a typical experiment in vapor phase, **CP5** (10 mg) was subjected to  $I_2$  vapor in a closed container for 1 day at room temperature. Brown solid **CP5** turned dark pink (nearly black in naked eyes) solid **CP5@I<sub>2</sub>(vapor)** which was thoroughly washed with pet ether to remove excess  $I_2$  adhered to the surface of the powdered sample of **CP5**. The amount of  $I_2$  adsorbed by **CP5** was quantified by thermogravimetric analysis (TGA) that showed 21.4 wt % adsorption. Thus, per formulae unit of **CP5** was able to adsorb ~0.6 molecules of  $I_2$ . The data were comparable to that observed for many reported

CPs.<sup>65,66</sup> In solution phase, **CP5** (10 mg) was kept immersed in  $I_2$  solution in pet ether (3 mL, 5 mmol) in a closed container for 1 day. Once again visual observation (turning dark pink  $I_2$  solution to light pink) was indicative of  $I_2$  adsorption. The  $I_2$  adsorbed solid **CP5@I<sub>2</sub>(solution)** was then filtered and washed several times with pet ether to remove adhered  $I_2$ . TGA data indicated that 30.3 wt % adsorption of  $I_2$  by **CP5** was achieved in solution phase. The value attributed to ~0.9 molecule of  $I_2$  adsorbed per formulae unit of **CP5**. The data were found consistent with that displayed by quite a few CPs.<sup>65–68</sup> (Figure 7)

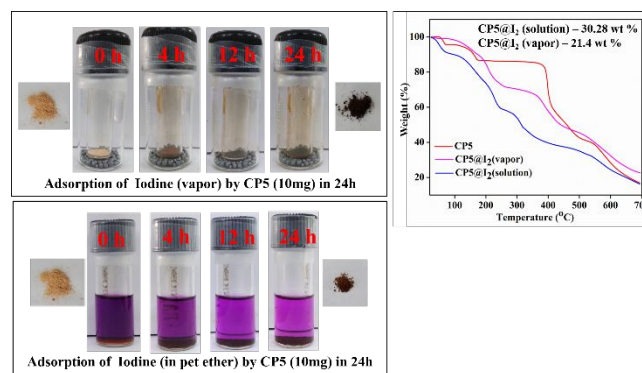


**Figure 7.** visual observation of  $I_2$  adsorption and TGA profile of  $I_2$  release.

FT-IR spectrum of **CP5**, **CP5@I<sub>2</sub>(vapor)** and **CP5@I<sub>2</sub>(solution)** were compared; the spectra were nearly superimposable suggesting weak interactions of  $I_2$  with **CP5**. PXRD patterns of as synthesized **CP5**, **CP5@I<sub>2</sub>(vapor)** and **CP5@I<sub>2</sub>(solution)** were also compared; all the patterns were in good agreement indicating no phase change due to  $I_2$  adsorption which further supported physical adsorption of  $I_2$  through weak interactions (Figure 8).

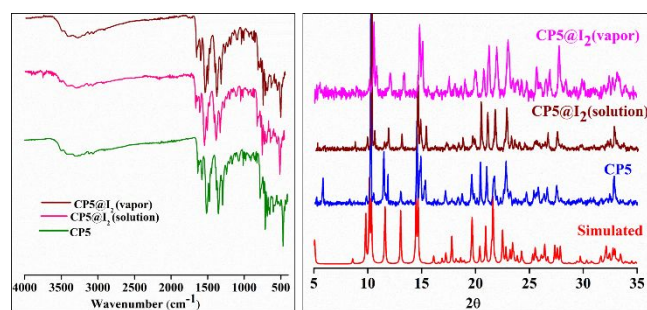


**Figure 8.** FT-IR and PXRD of **CP5** under various conditions.

Release of  $I_2$  from the iodine adsorbed **CP5** (both phases) was easy and spontaneous in polar organic solvents like EtOH. For this purpose, 1 mg of **CP5@I<sub>2</sub>(vapor)/CP5@I<sub>2</sub>(solution)** was immersed in 3 mL of EtOH. Colorless EtOH layer gradually turned brown within 4 h. *In situ* UV-vis absorption showed linear increase of the absorbance at 220–400 nm suggesting steady release of  $I_2$  from iodine adsorbed **CP5** (Figures S32–33, supporting information)

**Synthesis of Ag nanoparticles within the gel matrix of L1.**

We also considered exploring the possibility of generating metal nanoparticles (MNPs) in the gel matrix of **L1**. Owing to their quantum-size effects and large surface-to-volume ratio, MNPs are promising materials for catalysis.<sup>69</sup> Although access to MNPs is usually through reduction of a target metal salt with the help of external reducing agent, supramolecular gels wherein the gelator molecules have amide/urea/thiourea moieties are known to produce MNPs *in situ* without the help of exogenous reducing agent.<sup>70,71,72</sup> For generating silver nanoparticles, aqueous solution of AgNO<sub>3</sub> (2 mg in 2 mL of water) was placed over a gel bed of **L1** in DMSO/H<sub>2</sub>O (3:2). The solution was kept in dark at room temperature for 24 h. The color transition was observed from white opaque gel to light-brown gel indicating the formation of Ag nanoparticles (AgNPs) which were further studied by UV-vis and TEM. A peak at  $\lambda = 440$  nm in the UV-vis spectrum of gel containing MNP dispersed in DMSO at room temperature was due to the characteristic surface plasmon absorption band of AgNPs. FEG-TEM images of dried gel of **L1** containing AgNPs clearly showed that the MNPs were adhered to the surface of plate like gel networks. Presumably the bis-amide backbone of **L1** and visible light played a crucial role in reducing Ag ion to generate AgNPs within the gel matrix (Figure 9).

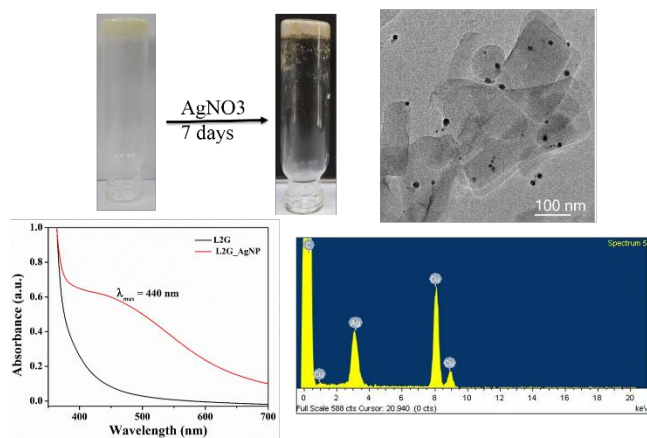


**Figure 9.** (clockwise) Synthesis of AgNPs in gel matrix of **L1**; TEM images of AgNPs adhered to the gel network; EDX displaying existence of Ag; typical surface plasmon spectra of AgNPs.

and **L2**. The results presented here clearly emphasized the importance of structural rationale based on which the CPs were designed. All the CPs (**CP1A-CP5**) were LOCS and the corresponding reactants under suitable conditions produced metallo gels (**MG1, MG2, MG4** and **MG5**) as envisaged. One of the CPs namely **CP5** displayed the ability to adsorb and release I<sub>2</sub> from

both vapor and solution phase. Thus a series of CPs was achieved that displayed multi-functional properties like metallogelation and molecular iodine adsorption. The aqueous gel of **L1** was also able to produce AgNPs without the help of any exogenous reducing agent.

## Experimental Section

**Materials and Methods for Physical Measurements.** All reagents and chemicals are purchased from commercial sources and used without further purification. FT-IR spectra were recorded on a FT-IR instrument (Perkin Elmer, FT-IR Spec-trometer, Spectrometer Two). Elemental analyses were performed on Perkin Elmer Precisely, Series-II, CHNO/S Analyser-2400. TGA experiments were done on a SDT Q Series 600 Uni-versal VA.2E TA instrument. X-ray powder diffraction patterns were recorded on a Bruker AXS D8 Advance Powder (CuK $\alpha$  radiation,  $\lambda = 1.5418$  Å) X-ray diffractometer. TEM images were recorded using a JEOL instrument (JEM-2100F; JEM-2010) with 300 mesh copper TEM grid. UV/Vis spectroscopic measurements were performed on a Hewlett-Packard 8453 diode array spectro-photometer equipped with a Peltier temperature controller. NMR spectra were carried out using 400/500 MHz spectrometer (Bruker Ultrashield Plus- 400/500).

**Synthesis of **L1**.** Nicotinoyl Chloride hydrochloride (1.78 g, 10 mmol) and dry triethyl amine (1.5 mL) were dissolved in dry DCM (250 mL) in a round bottom flask (500 mL). Then 4,4'-methylenedianiline (1 g, 5 mmol) in dry DCM (5 mL) were added drop wise under nitrogen atmosphere and the reaction mixture was stirred for 12 h at reflux temperature. Obtained precipitate was filtered and washed several times with dry DCM. The ligand **L2** was isolated (Yield 67%) as white precipitate followed by drying in vacuum.

**L1:** <sup>1</sup>H NMR (500 MHz, DMSO)  $\delta$  10.39 (s, 1H), 9.09 (s, 1H), 8.75 (d, J = 5 Hz, 1H), 8.28 (d, J = 5 Hz, 1H), 7.69 (d, J = 10 Hz, 1H), 7.56 (dd, J = 10, 5 Hz, 1H), 7.23 (d, J = 10 Hz, 1H), 3.91 (s, 2H) (see supporting information Figure S1); <sup>13</sup>C NMR (100 MHz, DMSO)  $\delta$  163.87, 152.02, 148.59, 137.11, 136.79, 135.34, 130.59, 129.07, 128.85, 123.48, 120.53 (see supporting information Figure S1). ESI-MS-(MeOH): calculated for [M+H]<sup>+</sup> is 409.16, found 409.08 (see supporting information Figure S3). FT-IR ( $\tilde{\nu}$ , cm<sup>-1</sup>): 3347, 1662, 1645, 1598, 1525, 1511, 1407, 1287, 1267, 820, 740, 706, 688, 511 (see the Supporting Information, Figure S4).

### Synthesis of the Coordination Polymers.

$[[\text{Cd}(\mu\text{-L1})(\mu\text{-TA})(\text{H}_2\text{O})_2] \cdot 3\text{H}_2\text{O} \cdot \text{MeOH}]_{\infty}$  (**CP1A**): A mixture of **L1** (20 mg, 0.05 mmol) and disodium terephthalate (Na<sub>2</sub>TA; 10 mg, 0.05 mmol) in DMF (2 mL) and MeOH (2 mL) was added to an aqueous solution (1 mL) of Cd(NO<sub>3</sub>)<sub>2</sub>·4H<sub>2</sub>O (15 mg, 0.05 mmol) in screw capped plastic vial (25 mL) and heated at 80 °C for 48 h in an oven. The mixture was slowly cooled to rt. and

colorless block-shaped crystals were formed, which were filtered and dried in air. FT-IR ( $\tilde{\nu}$ ,  $\text{cm}^{-1}$ ): 3270, 1658, 1604, 1538, 1505, 1410, 1376, 1325, 1047, 827, 753, 509.

$[\{\text{Cd}(\mu\text{-L1})(\mu\text{-TA})(\text{H}_2\text{O})\} \cdot \text{MeOH}]_{\infty}$  (**CP1B**): A mixture of L1 (20 mg, 0.05 mmol) and disodium terephthalate ( $\text{Na}_2\text{TA}$ ; 10 mg, 0.05 mmol) in DMF (1 mL) and MeOH (2 mL) was added to an aqueous solution (3 mL) of  $\text{Cd}(\text{NO}_3)_2 \cdot 4\text{H}_2\text{O}$  (15 mg, 0.05 mmol) in screw capped plastic vial (25 mL) and heated at  $80^\circ\text{C}$  for 48 h in an oven. The mixture was slowly cooled to rt. and colorless block-shaped crystals were formed, which were filtered and dried in air. FT-IR ( $\tilde{\nu}$ ,  $\text{cm}^{-1}$ ): 3292, 1662, 1608, 1544, 1506, 1410, 1385, 1328, 1051, 823, 775, 754, 513.

$[\{\text{Ni}(\mu\text{-L1})(\mu\text{-TA})(\text{H}_2\text{O})_2\} \cdot 3\text{H}_2\text{O} \cdot \text{MeOH}]_{\infty}$  (**CP2A**): CP2A was synthesized by following the procedure used for synthesizing CP1A; in this case,  $\text{Ni}(\text{NO}_3)_2 \cdot 6\text{H}_2\text{O}$  (14.5 mg, 0.05 mmol) was used. Upon slow cooling to rt., green block shape crystals were formed, which were filtered and dried in open air. FT-IR ( $\tilde{\nu}$ ,  $\text{cm}^{-1}$ ): 3304, 1673, 1603, 1541, 1510, 1482, 1377, 1326, 1017, 752, 696, 597, 507).

$[\{\text{Ni}(\mu\text{-L1})(\mu\text{-TA})(\text{H}_2\text{O})_2\} \cdot 4\text{H}_2\text{O} \cdot \text{MeOH}]_{\infty}$  (**CP2B**): CP2B was synthesized by following the procedure used for synthesizing CP1B; in this case  $\text{Ni}(\text{NO}_3)_2 \cdot 6\text{H}_2\text{O}$  (14.5 mg, 0.05 mmol) was used. Upon slow cooling to rt., green block shape crystals were formed, which were filtered, washed with MeOH and dried in open air. FT-IR ( $\tilde{\nu}$ ,  $\text{cm}^{-1}$ ): 3300, 1657, 1603, 1548, 1502, 1377, 1323, 1035, 832, 753, 505.

$[\{\text{Cu}(\mu\text{-L1})(\mu\text{-TA})(\text{H}_2\text{O})_2\} \cdot 3\text{H}_2\text{O}]_{\infty}$  (**CP3**): CP3 was synthesized by following the procedure used for synthesizing CP1A; in this case  $\text{Cu}(\text{NO}_3)_2 \cdot 3\text{H}_2\text{O}$  (12 mg, 0.05 mmol) was used. Upon slow cooling to rt., blue colored block shape crystals were formed, which were filtered and washed with MeOH and dried in open air. FT-IR ( $\tilde{\nu}$ ,  $\text{cm}^{-1}$ ): 3389, 1661, 1604, 1543, 1505, 1410, 1367, 1327, 1056, 826, 776, 751, 512.

$[\{\text{Zn}(\mu\text{-L1})(\mu\text{-TA})(\text{H}_2\text{O})_2\} \cdot 3\text{H}_2\text{O} \cdot \text{MeOH}]_{\infty}$  (**CP4**): CP4 was synthesized by following the procedure used for synthesizing CP1A; in this case  $\text{Zn}(\text{NO}_3)_2 \cdot 6\text{H}_2\text{O}$  (15 mg, 0.05 mmol) was used. Upon slow cooling to rt., colorless block shape crystals were formed, which were filtered and washed with MeOH and dried in open air. FT-IR ( $\tilde{\nu}$ ,  $\text{cm}^{-1}$ ): 3313, 1664, 1609, 1505, 1374, 1330, 1198, 824, 755, 642, 511.

$[\{\text{Co}(\mu\text{-L1})(\mu\text{-TA})(\text{MeOH})(\text{H}_2\text{O})\} \cdot \text{H}_2\text{O} \cdot \text{MeOH}]_{\infty}$  (**CP5**): CP5 was synthesized by following the procedure used for synthesizing CP1A; in this case  $\text{Co}(\text{NO}_3)_2 \cdot 6\text{H}_2\text{O}$  (14.5 mg, 0.05 mmol) was used. Upon slow cooling to rt., pink colored block shape crystals were formed, which were filtered and washed with MeOH and dried in open air. FT-IR ( $\tilde{\nu}$ ,  $\text{cm}^{-1}$ ): 3283, 1660, 1605, 1542, 1503, 1383, 1326, 1275, 1048, 751, 512.

**Gelation.** L1 (40 mg) was dissolved in DMSO (0.6 mL) in a glass vial (3 mL) by heating on a hot plate. The solution was cooled to rt. to which water (0.4 mL) was added resulting in instant gelation (MGC 4 wt %) as evident from tube inversion and rheological data. It was found to be thermoreversible over a few cycles.

**Metallogelation.** A clear solution of L1 in DMF was mixed with an aqueous solution containing  $\text{Na}_2\text{TA}$  and the corresponding metal salt in a sonicator (5-10 mins) at ambient condition that resulted in metallogel.

**Transmission electron Microscopy.** Small amount of gel sample was smeared on a 300 mesh Cu grid and dried under vacuum at room temperature for 1 day. TEM images were recorded without staining.

**Single Crystal X-ray Crystallography.** Single crystal X-ray data were collected by using Moka ( $\lambda=0.7107\text{\AA}$ ) radiation on a BRUKER APEX II diffractometer equipped with CCD area detector. Data collection and data reduction were done using APEX II package software. The structures were solved by using direct methods and refined in a routine manner. Data of **CP2A** and **CP3** were collected in Bruker D8VENTURE Micro focus diffractometer equipped with PHOTON II detector ( $\text{Mo } \alpha$  ( $\lambda=0.7107\text{\AA}$ )). Data collection and data reduction were done by using APEX3 software package in a routine manner. Final refinement and CIF finalization were carried out by using OLEX2 version 1.2.9. In all cases, the non-hydrogen atoms were treated anisotropically whereas most of the hydrogen atoms were geometrically fixed; wherever possible, the hydrogen atoms associated with guest solvent molecules were located on difference Fourier map and refined. CIFs files has been deposited to The Cambridge Crystallographic Data Centre (CCDC). CCDC 1863205-1863211 contain the supplementary crystallographic data for this paper. These data can be obtained free of charge from CCDC.

**Powder X-ray Diffraction.** A thin layer made on a glass slide from bulk powdered sample (~15 mg) was used for data collection using Bruker AXS D8 Advanced powder diffractometer ( $\text{Cu } \alpha$  radiation,  $\lambda=1.5406\text{\AA}$ ) equipped with super speed LYNXEXE detector with a scan speed 0.3 sec/step for scan range of  $2\theta(5^\circ-35^\circ)$ .

## ASSOCIATED CONTENT

**Supporting Information.** Supporting information is available free of charge via the Internet at <http://pubs.acs.org>.

$^1\text{H}$ ,  $^{13}\text{C}$  NMR, FT-IR, HRMS, ORTEP plots, hydrogen bonding table, TGA, PXRD patterns, Rheological data, UV-vis spectra.

Author information

Corresponding author

\*E-mail: [ocpd@iacs.res.in](mailto:ocpd@iacs.res.in)

## ACKNOWLEDGMENT

SM thanks UGC for research fellowship. P.D. thanks DST (Grant No. EMR/2016/000894) for financial support. P.D. indebted to Professor Israel Goldberg for giving him opportunity to work as a post-doctoral fellow under his supervision during the year 1994-1996.

## REFERENCES

- (1) Terech, P.; Weiss, R. G. Low Molecular Mass Gelators of Organic Liquids and the Properties of Their Gels. *Chem. Rev.* **1997**, *97*, 3133–3160.
- (2) Smith, D. K. Building Bridges. *Nat. Chem.* **2010**, *2*, 162–163.
- (3) Draper, E. R.; Adams, D. J. How should multicomponent supramolecular gels be characterised? *Chem. Soc. Rev.* **2018**, *47*, 3395–3405.
- (4) Suzuki, M.; Hanabusa, K. L-Lysine-based low-molecular-weight gelators. *Chem. Soc. Rev.* **2009**, *38*, 967–975.
- (5) Segarra-Maset, M. D.; Nebot, V. J.; Miravet, J. F.; Escuder, B. Control of molecular gelation by chemical stimuli. *Chem. Soc. Rev.* **2013**, *42*, 7086–7098.
- (6) Babu, S. S.; Praveen, V. K.; Ajayaghosh, A. Functional  $\pi$ -Gelators and Their Applications. *Chem. Rev.* **2014**, *114*, 1973–2129.
- (7) Van Bommel, K. J. C.; Friggeri, A.; Shinkai, S. Organic Templates for the Generation of Inorganic Materials. *Angew. Chem. Int. Ed.* **2003**, *42*, 980–999.
- (8) Majumder, J.; Dastidar, P. An Easy Access to Organic Salt-Based Stimuli-Responsive and Multifunctional Supramolecular Hydrogels. *Chem. Eur. J.* **2016**, *22*, 9267–9276.
- (9) Bhattacharya, S.; Ghosh, Y. K. First report of phase selective gelation of oil from oil/water mixtures. Possible implications toward containing oil spills. *Chem. Commun.* **2001**, 185–186.
- (10) Carretti, E.; Bonini, M.; Dei, L.; Berrie, B. H. New Frontiers in Materials Science for Art Conservation: Responsive Gels and Beyond. *Acc. Chem.* **2010**, *43*, 751–760.
- (11) Feringa, B. L.; de Jong, J. J. D.; Lucas, L. N.; Kellogg, R. M.; van Esch, J. H. Reversible Optical Transcription of Supramolecular Chirality into Molecular Chirality. *Science* **2004**, *304*, 278–281.
- (12) Hirst, A. R.; Escuder, B.; Miravet, J. F.; Smith, D. K. High-Tech Applications of Self-Assembling Supra-molecular Nanostructured Gel-Phase Materials: From Regenerative Medicine to Electronic Devices. *Angew. Chem. Int. Ed.* **2008**, *47*, 8002–8018.
- (13) George, M.; Weiss, R. G. Molecular Organogels. Soft Matter Comprised of Low-Molecular-Mass Organic Gelators and Organic Liquids. *Acc. Chem. Res.* **2006**, *39*, 489–497.
- (14) Xing, B.; Choi, M.-F.; Xu, B. A stable metal coordination polymer gel based on a calix[4]arene and its 'uptake' of non-ionic organic molecules from the aqueous phase. *Chem. Commun.* **2002**, 362–363.
- (15) Steed, J. W. Anion-tuned supramolecular gels: a natural evolution from urea supramolecular chemistry. *Chem. Soc. Rev.* **2010**, *39*, 3686–3699.
- (16) Dastidar, P.; Ganguly, S.; Sarkar, K. Metallogels from Coordination Complexes, Organometallic, and Coordination Polymers. *Chem. Asian J.* **2016**, *11*, 2484–2498.
- (17) Tam, A. Y.-Y.; Yam, V. W.-W. Recent advances in metallogels. *Chem. Soc. Rev.* **2013**, *42*, 1540–1567.
- (18) Feldner, T.; H-ring, M.; Saha, S.; Esquena, J.; Banerjee, R.; Diaz, D. D. Supramolecular Metallogel That Imparts Self-Healing Properties to Other Gel Networks. *Chem. Mater.* **2016**, *28*, 3210–3217.
- (19) Byrne, P.; Lloyd, G. O.; Applegarth, L.; Anderson, K. M.; Clarke, N.; Steed, J. W. Metal-induced gelation in dipyriddy ureas. *New J. Chem.*, **2010**, *34*, 2261–2274.
- (20) Ljpez, D.; Guenet, J. M. Behavior of a Self-Assembling Bicopper Complex in Organic Solutions. *Macromolecules* **2001**, *34*, 1076–1081.
- (21) Ishi-i, T.; Iguchi, I. R.; Snip, E.; Ikeda, M.; Shinkai, S. [60]Fullerene Can Reinforce the Organogel Structure of Porphyrin-Appended Cholesterol Derivatives: Novel Odd-Even Effect of the (CH<sub>2</sub>)<sub>n</sub> Spacer on the Organogel Stability. *Langmuir* **2001**, *17*, 5825–5833.
- (22) Kimura, M.; Muto, T.; Takimoto, H.; Wada, K.; Ohta, K.; Hanabusa, K.; Shirai, H.; Kobayashi, N. Fibrous Assemblies Made of Amphiphilic Metallophthalocyanines. *Langmuir* **2000**, *16*, 2078–2082.
- (23) Hanabusa, K.; Maesaka, Y.; Suzuki, M.; Kimura, M.; Shirai, H. Low Molecular Weight Gelator Containing  $\beta$ -Diketonato Ligands: Stabilization of Gels by Metal Coordination. *Chem. Lett.* **2000**, *29*, 1168–1169.
- (24) Rajeev Kumar, V. R.; Sajini, V.; Sreeprasad, T. S.; Praveen V. K.; Ajayaghosh, A.; Pradeep, T. Probing the Initial Stages of Molecular Organization of Oligo(p-phenylenevinylene) Assemblies with Monolayer Protected Gold Nanoparticles. *Chem. Asian J.* **2009**, *4*, 840–848.
- (25) Zhu, L.; Li, X.; Wu, S.; Nguyen, K. T.; Yan, H.; agren, H.; Zhao, Y. Chirality Control for in Situ Preparation of Gold Nanoparticle Superstructures Directed by a Coordinatable Organogelator. *J. Am. Chem. Soc.* **2013**, *135*, 9174–9180.
- (26) Biswas, P.; Ganguly, S.; Dastidar, P. Stimuli-Responsive Metallogels for Synthesizing Ag Nanoparticles and Sensing Hazardous Gases. *Chem. Asian J.* **2018**, *13*, 1914–1949.
- (27) Adarsh, N. N.; Kumar, D. K.; Dastidar, P. Composites of N,N'-bis-(pyridyl) urea-dicarboxylic acid as new hydrogelators—a crystal engineering approach. *Tetrahedron* **2007**, *63*, 7386–7396.
- (28) Tu, T.; Fang, W.; Bao, X.; Li, X.; Dçtz, K. H. Visual Chiral Recognition through Enantioselective Metallogel Collapsing: Synthesis, Characterization, and Application of Platinum-Steroid Low-Molecular-Mass Gelators. *Angew. Chem. Int. Ed.* **2011**, *50*, 6601–6605.
- (29) Li, J. L.; Liu, X. Y. Architecture of Supramolecular Soft Functional Materials: From Understanding to Micro-/Nanoscale Engineering. *Adv. Funct. Mater.* **2010**, *20*, 3196–3216.
- (30) Lan, Y.; Corradini, M. G.; Weiss, R. G.; Raghavan, S. R.; Rogers, M. A. To gel or not to gel: correlating molecular gelation with solvent parameters. *Chem. Soc. Rev.* **2015**, *44*, 6035–6058.
- (31) James, S. L.; Lloyd, G. O.; Zhang, J. Supramolecular gels in crystal engineering. *CrystEngComm* **2015**, *17*, 7976–7977.
- (32) Dastidar, P. Supramolecular gelling agents: can they be designed? *Chem. Soc. Rev.* **2008**, *37*, 2699–2715.
- (33) Roy, R.; Parveen, R.; Sarkar, K.; Dastidar, P. Supramolecular Synthon Approach in Designing Molecular Gels for Advanced Therapeutics. *Adv. Therap.* **2018**, 1800061.
- (34) Kumar, D. K.; Jose, D. A.; Dastidar, P.; Das, A. Nonpolymeric Hydrogelators Derived from Trimesic Amides. *Chem. Mater.* **2004**, *16*, 2332–2335.
- (35) Kumar, D. K.; Jose, D. A.; Das, A.; Dastidar, P. First snapshot of a nonpolymeric hydrogelator interacting with its gelling solvents. *Chem. Commun.* **2005**, 4059–4061.
- (36) Kiyonaka, S.; Sada, K.; Yoshimura, I.; Shinkai, S.; Kato, N.; Hamachi, I. Semi-wet peptide/protein array using supramolecular hydrogel. *Nat. Mater.* **2004**, *3*, 58–64.
- (37) Adarsh, N. N.; Sahoo, P.; Dastidar, P. Is a Crystal Engineering Approach Useful in Designing Metallogels? A Case Study. *Cryst. Growth Des.* **2010**, *10*, 4976–4986.
- (38) Adarsh, N. N.; Dastidar, P. A New Series of ZnII Coordination Polymer Based Metallogels Derived from Bis-pyridyl-bis-amidenLigands: A Crystal Engineering Approach. *Cryst. Growth Des.* **2011**, *11*, 328–336.
- (39) Lebel, O.; Perron, M.; Maris, T.; Zalzal, S. F.; Nanci, A.; Wuest J. D. A New Class of Selective Low-Molecular-Weight Gelators Based on Salts of Diaminotriazinecarboxylic Acids. *Chem. Mater.* **2006**, *18*, 3616–3626.
- (40) Carpenter, L. J. Iodine in the Marine Boundary Layer. *Chem. Rev.* **2003**, *103*, 4953–4962.
- (41) Huang, R. J.; Hoffmann, T. Development of a Coupled Diffusion Denuder System Combined with Gas Chromatography/Mass Spectrometry for the Separation and Quantification of Molecular Iodine and the Activated Iodine Compounds Iodine Monochloride and Hypoiodous Acid in the Marine Atmosphere. *Anal. Chem.* **2009**, *81*, 1777–1783.
- (42) Smyth, PPA. The thyroid, iodine and breast cancer. *Breast Cancer Res.* **2003**, *5*, 235–238.
- (43) Rubinstein, I.; Gileadi, E. Measurement of electrical conductivity in solid bromine and iodine. *J. Electroanal. Chem.* **1980**, *108*, 191–201.
- (44) Falaise, C.; Volkringer, C.; Facqueur, J.; Bousquet, T.; Gasnot, L.; Loiseau, T. Capture of iodine in highly stable metal-organic frameworks: a systematic study. *Chem. Commun.* **2013**, *49*, 10320–10322. (reference cited therein)

- (45) Sava, D. F.; Chapman, K. W.; Rodriguez, M. A.; Greathouse, J. A.; Crozier, P. S.; Zhao, H.; Chupas, P. J.; Nenoff, T. M. Competitive I<sub>2</sub> Sorption by Cu-BTC from Humid Gas Streams. *Chem. Mater.* **2013**, *25*, 2591–2596. (reference cited therein)
- (46) Massasso, G.; Long, J. r. m.; Haines, J.; Devautour-Vinot, S.; Maurin, G.; Grandjean, A. s.; Onida, B.; Donnadiou, B.; Larionova, J.; Guérin, C.; Guari, Y. Iodine Capture by Hofmann-Type Clathrate NiII(pz)[NiII(CN)<sub>4</sub>]. *Inorg. Chem.* **2014**, *53*, 4269–4271. (reference cited therein)
- (47) Sava, D. F.; Garino, T. J.; Nenoff, T. M. Iodine Confinement into MetalOrganic Frameworks (MOFs): Low-Temperature Sintering Glasses To Form Novel Glass Composite Material (GCM) Alternative Waste Forms. *Ind. Eng. Chem. Res.* **2012**, *51*, 614–620. (reference cited therein)
- (48) Wang, J.; Luo, J. H.; Luo, X. L.; Zhao, J.; Li, D.-S.; Li, G. H.; Huo, Q. S.; Liu, Y. L. Assembly of a Three-Dimensional Metal–Organic Framework with Copper(I) Iodide and 4-(Pyrimidin-5-yl) Benzoic Acid: Controlled Uptake and Release of Iodine. *Cryst. Growth Des.* **2015**, *15*, 915–920. (reference cited therein)
- (49) Subrahmanyam, K. S.; Malliakas, C. D.; Sarma, D.; Armatas, G. S.; Wu, J.; Kanatzidis, M. G. Ion-Exchangeable Molybdenum Sulfide Porous Chalcogel: Gas Adsorption and Capture of Iodine and Mercury. *J. Am. Chem. Soc.* **2015**, *137*, 13943–13948.
- (50) Bennett, T. D.; Saines, P. J.; Keen, D. A.; Tan, J.-C.; Cheetham, A. K. Ball-Milling-Induced Amorphization of Zeolitic Imidazolate Frameworks (ZIFs) for the Irreversible Trapping of Iodine. *Chem. - Eur. J.* **2013**, *19*, 7049–7055.
- (51) Katsoulidis, A. P.; He, J.; Kanatzidis, M. G. Functional Monolithic Polymeric Organic Framework Aerogel as Reducing and Hosting Media for Ag nanoparticles and Application in Capturing of Iodine Vapors. *Chem. Mater.* **2012**, *24*, 1937–1943.
- (52) Zeng, M.-H.; Wang, Q.-X.; Tan, Y.-X.; Hu, S.; Zhao, H.-X.; Long, L.-S.; Kurmoo, M. Rigid Pillars and Double Walls in a Porous Metal–Organic Framework: Single-Crystal to Single-Crystal, Controlled Uptake and Release of Iodine and Electrical Conductivity. *J. Am. Chem. Soc.* **2010**, *132*, 2561–2563.
- (53) Zeng, M.-H.; Yin, Z.; Tan, Y.-X.; Zhang, W.-X.; He, Y.-P.; Kurmoo, M. Nanoporous Cobalt(II) MOF Exhibiting Four Magnetic Ground States and Changes in Gas Sorption upon Post-Synthetic Modification. *J. Am. Chem. Soc.* **2014**, *136*, 4680–4688.
- (54) Sun, F.; Yin, Z.; Wang, Q.-Q.; Sun, D.; Zeng, M.-H.; Kurmoo, M. Tandem Postsynthetic Modification of a Metal–Organic Framework by Thermal Elimination and Subsequent Bromination: Effects on Adsorption Properties and Photoluminescence. *Angew. Chem., Int. Ed.* **2013**, *52*, 4538–4543.
- (55) Yin, Z.; Zhou, Y.-L.; Zeng, M.-H.; Kurmoo, M. The Concept of Mixed Organic Ligands in Metal–Organic Frameworks: Design, Tuning and Functions. *Dalton Trans.* **2015**, *44*, 5258–5275.
- (56) Dang, Q.-Q.; Wang, X.-M.; Zhan, Y.-F.; Zhang, X.-M. Azolinked Porous Triptycene Network as adsorbents for CO<sub>2</sub> and iodine uptake. *Polym. Chem.* **2016**, *7*, 643–647.
- (57) Chen, Y.; Sun, H.; Yang, R.; Wang, T.; Pei, C.; Xiang, Z.; Zhu, Z.; Liang, W.; Li, A.; Deng, W. Synthesis of conjugated microporous polymer nanotubes with large surface areas as adsorbents for iodine and CO<sub>2</sub> uptake. *J. Mater. Chem. A* **2015**, *3*, 87–91.
- (58) Sava, D. F.; Rodriguez, M. A.; Chapman, K. W.; Chupas, P. J.; Greathouse, J. A.; Crozier, P. S.; Nenoff, T. M. Capture of Volatile Iodine, a Gaseous Fission Product, by Zeolitic Imidazolate Framework-8. *J. Am. Chem. Soc.* **2011**, *133*, 12398–12401.
- (59) (a) Hughes, J. T.; Sava, D. F.; Nenoff, T. M.; Navrotsky, A. Thermochemical Evidence for Strong Iodine Chemisorption by ZIF-8. *J. Am. Chem. Soc.* **2013**, *135*, 16256–16259.
- (60) Yin, Z.; Wang, Q.; Zeng, M. H. Iodine Release and Recovery, Influence of Polyiodide Anions on Electrical Conductivity and Nonlinear Optical Activity in an Interdigitated and Interpenetrated Bipillared-Bilayer Metal–Organic Framework. *J. Am. Chem. Soc.* **2012**, *134*, 4857–4863.
- (61) Wang, Z.; Zhang, Y.; Liu, T.; Kurmoo, M.; Gao, S. [Fe<sub>3</sub>(HCOO)<sub>6</sub>]: A Permanent Porous Diamond Framework Displaying H<sub>2</sub>/N<sub>2</sub> Adsorption, Guest Inclusion, and Guest-Dependent Magnetism. *Adv. Funct. Mater.* **2007**, *17*, 1523–1536.
- (62) Alexandrov, E. V.; Blatov, V. A.; Kochetkov, A. V.; Proserpio, D. M. Underlying nets in three-periodic coordination polymers: topology, taxonomy and prediction from a computer-aided analysis of the Cambridge Structural Database. *CrystEngComm* **2011**, *13*, 3947–3958.
- (63) Blatov, V. A. Nanocluster analysis of intermetallic structures with the program package TOPOS. *Struct. Chem.* **2012**, *23*, 955–963.
- (64) Ghosh, A.; Das, P.; Kaushik, R.; Damodaran, K. K.; Jose, D. A. Anion responsive and morphology tunable tripodal gelators. *RSC Adv.* **2016**, *6*, 83303–83311.
- (65) Arici, M.; Yeşilel, O. Z.; Tas, M.; Demiral, H. CO<sub>2</sub> and Iodine Uptake Properties of Co(II)-Coordination Polymer Constructed from Tetracarboxylic Acid and Flexible Bis(imidazole) Linker. *Cryst. Growth Des.* **2017**, *17*, 2654–2659.
- (66) Arici, M.; Yeşilel, O. Z.; Tas, M.; Demiral, H. Effect of Solvent Molecule in Pore for Flexible Porous Coordination Polymer upon Gas Adsorption and Iodine Encapsulation. *Inorg. Chem.* **2015**, *54*, 11283–11291.
- (67) Parshamoni, S.; Sanda, S.; Jena, H. S.; Konar, S. Tuning CO<sub>2</sub> Uptake and Reversible Iodine Adsorption in Two Isorecticular MOFs through Ligand Functionalization. *Chem. Asian J.* **2015**, *10*, 653–660.
- (68) Zhao, Si-Si.; Chen, Li.; Zheng, X.; Wang, L.; Xie, Z. PEG-Induced Synthesis of Coordination-Polymer Isomers with Tunable Architectures and Iodine Capture. *Chem. Asian J.* **2017**, *12*, 615–620.
- (69) Talapin, D.; Shevchenko, E. Introduction: Nanoparticle Chemistry. *Chem. Rev.* **2016**, *116*, 10343–10345.
- (70) Das, D.; Kar, T.; Das, P. K. Gel-nanocomposites: materials with promising applications. *Soft Matter*, **2012**, *8*, 2348–2365.
- (71) Vemula, P. K.; John, G. Smart amphiphiles: hydro/organogelators for in situ reduction of gold. *Chem. Commun.* **2006**, 2218–2220.
- (72) Piepenbrock, M. O. M.; Clarke, N.; Steed, J. W. Rheology and silver nanoparticle templating in a bis(urea) silver metallogel. *Soft Matter*, **2011**, *7*, 2412–2418.

1  
2  
3  
4  
5  
6  
7  
8  
9  
10  
11  
12  
13  
14  
15  
16  
17  
18  
19  
20  
21  
22  
23  
24  
25  
26  
27  
28  
29  
30  
31  
32  
33  
34  
35  
36  
37  
38  
39  
40  
41  
42  
43  
44  
45  
46  
47  
48  
49  
50  
51  
52  
53  
54  
55  
56  
57  
58  
59  
60

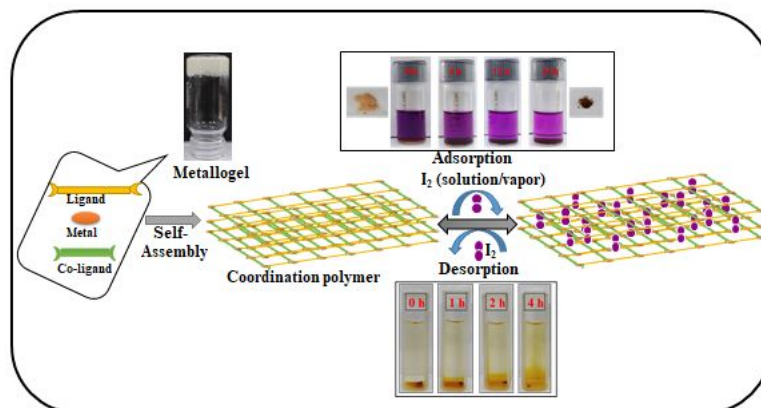
Table 1. Crystallographic data and structure-refinement parameters for polymers CP1A–CP5.

Identification code	CP1A	CP1B	CP2A	CP2B	CP3	CP4	CP5
CCDC	1863206	1863211	1863210	1863205	1863207	1863208	1863209
Empirical formula	C <sub>33.5</sub> H <sub>26</sub> CdN <sub>4</sub> O <sub>11.25</sub>	C <sub>34</sub> H <sub>30</sub> CdN <sub>4</sub> O <sub>8</sub>	C <sub>34</sub> H <sub>30</sub> N <sub>4</sub> NiO <sub>11</sub>	C <sub>34</sub> H <sub>24</sub> N <sub>4</sub> NiO <sub>13</sub>	C <sub>33</sub> H <sub>28</sub> CuN <sub>4</sub> O <sub>11</sub>	C <sub>33.25</sub> H <sub>28</sub> N <sub>4</sub> O <sub>11.5</sub> Zn	C <sub>35</sub> H <sub>30</sub> CoN <sub>4</sub> O <sub>10</sub>
Formula weight	776.98	735.02	729.33	755.28	720.13	732.96	725.56
Temperature/K	296.15	296.15	142.81	100.01	298	298	120.22
Crystal system	triclinic	orthorhombic	monoclinic	triclinic	triclinic	triclinic	triclinic
Space group	P-1	Pbca	C2/c	P-1	P-1	P-1	P-1
a/Å	9.539(6)	11.4197(15)	18.505(8)	9.2545(10)	9.2658(8)	9.389(6)	9.3588(4)
b/Å	11.408(7)	20.410(3)	18.012(8)	11.1448(12)	11.0361(9)	11.324(7)	11.2448(5)
c/Å	17.330(11)	26.422(4)	21.407(9)	17.409(2)	17.4680(13)	17.511(11)	17.4321(7)
α/°	85.615(10)	90	90	92.728(4)	92.978(3)	92.451(9)	91.987(3)
β/°	85.125(10)	90	111.239(6)	90.397(4)	90.487(3)	90.647(9)	90.278(3)
γ/°	66.829(9)	90	90	113.308(4)	114.101(2)	113.400(9)	113.882(3)
Volume/Å <sup>3</sup>	1725.5(19)	6158.3(14)	6651(5)	1646.5(3)	1627.5(2)	1706.4(19)	1676.08(13)
Z	2	8	8	2	2	2	2
ρ <sub>calc</sub> /cm <sup>3</sup>	1.495	1.586	1.457	1.523	1.47	1.427	1.438
μ/mm <sup>-1</sup>	0.698	0.77	0.651	0.665	0.739	0.787	0.577
F(000)	786	2992	3024	776	742	755	750
Crystal size/mm <sup>3</sup>	0.36 × 0.15 × 0.1	0.3 × 0.21 × 0.12	0.28 × 0.16 × 0.12	0.31 × 0.22 × 0.15	0.9 × 0.32 × 0.2	0.25 × 0.12 × 0.08	0.34 × 0.25 × 0.18
Radiation	MoKα (λ = 0.71073)	MoKα (λ = 0.71073)	MoKα (λ = 0.71073)	MoKα (λ = 0.71073)	MoKα (λ = 0.71073)	MoKα (λ = 0.71073)	MoKα (λ = 0.71073)
2θ range for data collection/°	2.362 to 40.364	3.082 to 53.632	3.27 to 51.12	4.512 to 46.848	4.552 to 54.598	2.328 to 39.356	3.964 to 52.812
Index ranges	-9 ≤ h ≤ 9, -11 ≤ k ≤ 11, -16 ≤ l ≤ 16	-14 ≤ h ≤ 14, -25 ≤ k ≤ 25, -32 ≤ l ≤ 33	-22 ≤ h ≤ 22, -21 ≤ k ≤ 21, -25 ≤ l ≤ 25	-10 ≤ h ≤ 9, -11 ≤ k ≤ 12, -19 ≤ l ≤ 19	-11 ≤ h ≤ 11, -14 ≤ k ≤ 14, -20 ≤ l ≤ 22	-8 ≤ h ≤ 8, -10 ≤ k ≤ 10, -16 ≤ l ≤ 16	-11 ≤ h ≤ 11, -13 ≤ k ≤ 14, -21 ≤ l ≤ 21
Reflections collected	26304	75322	80080	14161	20088	15266	21989
Independent reflections	3297 [R <sub>int</sub> = 0.0958, R <sub>sigma</sub> = 0.0508]	6523 [R <sub>int</sub> = 0.0576, R <sub>sigma</sub> = 0.0354]	6210 [R <sub>int</sub> = 0.0923, R <sub>sigma</sub> = 0.0446]	4759 [R <sub>int</sub> = 0.0569, R <sub>sigma</sub> = 0.0696]	7271 [R <sub>int</sub> = 0.0868, R <sub>sigma</sub> = 0.1237]	3009 [R <sub>int</sub> = 0.0693, R <sub>sigma</sub> = 0.0514]	6808 [R <sub>int</sub> = 0.0869, R <sub>sigma</sub> = 0.1142]
Data/restraints/parameters	3297/0/448	6523/0/427	6210/0/461	4759/0/459	7271/0/443	3009/0/449	6808/4/446
Goodness-of-fit on F <sup>2</sup>	1.082	0.936	1.024	1.129	1.067	1.053	0.988
Final R indexes [I > 2σ(I)]	R <sub>1</sub> = 0.0545, wR <sub>2</sub> = 0.1523	R <sub>1</sub> = 0.0436, wR <sub>2</sub> = 0.2087	R <sub>1</sub> = 0.0444, wR <sub>2</sub> = 0.1165	R <sub>1</sub> = 0.0916, wR <sub>2</sub> = 0.2384	R <sub>1</sub> = 0.0898, wR <sub>2</sub> = 0.2220	R <sub>1</sub> = 0.0650, wR <sub>2</sub> = 0.2071	R <sub>1</sub> = 0.0685, wR <sub>2</sub> = 0.1757
Final R indexes [all data]	R <sub>1</sub> = 0.0726, wR <sub>2</sub> = 0.1684	R <sub>1</sub> = 0.0722, wR <sub>2</sub> = 0.2294	R <sub>1</sub> = 0.0800, wR <sub>2</sub> = 0.1409	R <sub>1</sub> = 0.1157, wR <sub>2</sub> = 0.2535	R <sub>1</sub> = 0.1570, wR <sub>2</sub> = 0.2666	R <sub>1</sub> = 0.0850, wR <sub>2</sub> = 0.2283	R <sub>1</sub> = 0.1229, wR <sub>2</sub> = 0.2097

**Table 2. Gelation and Rheology table of various metallo gels.**

Gel	Metal Salt	Ligand (L1)	Co-Ligand (TA)	MGC (wt%)	Critical Strain (%)	G'	G''/G'
MG1	Cd(NO <sub>3</sub> ) <sub>2</sub> ; 4.5 mg (0.014mmol)	6 mg (0.014mmol)	3 mg (0.014mmol)	5.4	7.74	2.37*10 <sup>5</sup>	0.24
MG2	Ni(NO <sub>3</sub> ) <sub>2</sub> ; 4.27 mg (0.014mmol)	6mg (0.014mmol)	3 mg (0.014mmol)	5.3	70.08	9.32*10 <sup>4</sup>	0.23
MG4	Zn(NO <sub>3</sub> ) <sub>2</sub> ; 4.4 mg (0.014mmol)	6 mg (0.014mmol)	3 mg (0.014mmol)	5.36	8.73	7.69*10 <sup>4</sup>	0.39
MG5	Co(NO <sub>3</sub> ) <sub>2</sub> ; 4.28 mg (0.014mmol)	6 mg (0.014mmol)	3 mg (0.014mmol)	5.31	7.01	2.03*10 <sup>3</sup>	0.42

1  
2  
3 SYNOPSIS TOC. A crystal engineering based approach has been adopted to generate a series of coordination  
4 polymers that displayed both metallogelation and I<sub>2</sub> adsorption  
5  
6  
7  
8  
9



36 Insert Table of Contents artwork here  
37  
38  
39  
40  
41  
42  
43  
44  
45  
46  
47  
48  
49  
50  
51  
52  
53  
54  
55  
56  
57  
58  
59  
60